

## Supramolecular Chemistry

## Emergent Catalytic Behavior of Self-Assembled Low Molecular Weight Peptide-Based Aggregates and Hydrogels

Marta Tena-Solsona,<sup>[a]</sup> Jayanta Nanda,<sup>[b]</sup> Santiago Díaz-Oltra,<sup>[a]</sup> Agata Chotera,<sup>[b]</sup> Gonen Ashkenasy,<sup>\*,[b]</sup> and Beatriu Escuder<sup>\*,[a]</sup>

**Abstract:** We report a series of short peptides possessing the sequence (FE)<sub>n</sub> or (EF)<sub>n</sub> and bearing L-proline at their N-terminus that self-assemble into high aspect ratio aggregates and hydrogels. We show that these aggregates are able to catalyze the aldol reaction, whereas non-aggregated analogues are catalytically inactive. We have undertaken an analysis of the results, considering the accessibility of catalytic sites, pK<sub>a</sub> value shifts, and the presence of hydrophobic pockets. We conclude that the presence of hydrophobic re-

gions is indeed relevant for substrate solubilization, but that the active site accessibility is the key factor for the observed differences in reaction rates. The results presented here provide an example of the emergence of a new chemical property caused by self-assembly, and support the relevant role played by self-assembled peptides in prebiotic scenarios. In this sense, the reported systems can be seen as primitive aldolase I mimics, and have been successfully tested for the synthesis of simple carbohydrate precursors.

## Introduction

The emergence of new functional properties following the self-assembly of small molecular components into supramolecular structures is fundamental to many applications in the fields of nanotechnology, catalysis, and nanomedicine. Such functions evolve due to the transfer of physicochemical information at the supramolecular level, and moreover as a result of developing synergistic features, such as multivalent substrate binding and cooperative reactivity.<sup>[1]</sup> In this sense, the most significant emergent event on earth, the emergence of life itself, has been postulated to have proceeded through the self-assembly of simple prebiotic molecular components. Several artificial protocell models have been consequently reported, based on the self-assembly of amphiphilic components into closed nanostructures (vesicles, capsules, polymersomes) encapsulating reactants and catalysts.<sup>[2]</sup> Alternatively, peptide membranes have also been proposed to play a role in chemical evolution, not only through the formation of closed vesicles, but also through other morphologies, such as hollow tubes, ribbons, and fibers.<sup>[3]</sup> In fact, in some recent reports, self-assembled fibrillar networks were advocated as the most applicable functional scaffolds for simple prebiotic systems.<sup>[4]</sup>

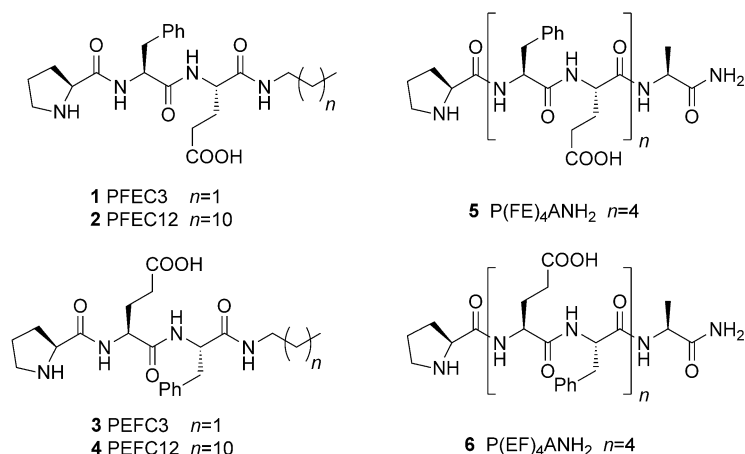
Fibrillar networks are also found in today's cellular environments, either as structural frameworks within the cell (i.e., actin), or as components of the extracellular matrix. Remarkably, these are also active components crucial for the cell life cycle, as in the case of microtubules that participate in cell motility and division. Besides their structural roles in creating compartments and isolating chemicals and processes from the environment, fibrillar assemblies can help in the co-localization of reactants and catalytic sites in a manner similar to enzymes, thus leading to supramolecular catalytic effects. It has been shown that the formation of arrays of functional groups on the surface of self-assembled nanostructures, such as micelles<sup>[5]</sup> and peptide hydrogel fibers,<sup>[6]</sup> may activate or enhance their catalytic efficiency. Moreover, as specific examples relevant to chemical evolution, short self-assembled peptides have been used to display efficient self-replication.<sup>[7]</sup>

With the aim of developing supramolecular systems that enable the emergence of additional catalytic properties so far found only in the natural counterparts, we present here an example of short peptides, each equipped with a catalytic functional group (Scheme 1), which forms fibrillar networks and hydrogels. We show that these networks are catalytically active for a C–C bond-forming reaction, the direct aldol coupling, whereas non-assembling analogues are inactive in solution, revealing the emergence of enamine-based catalysis through self-assembly. Moreover, the effect of subtle changes in the amino acid sequence on the catalytic efficiency is observed, suggesting the formation of tailored catalytic sites. Our networks represent a new example of a primitive system that could have acted as a proto-enzyme assisting the production of simple metabolite precursors. Indeed, C–C bond-forming reactions are crucial for the biosynthesis of many known metabolites. Aldolases (transaldolase, transketolase), for example, cat-

[a] Dr. M. Tena-Solsona, Dr. S. Díaz-Oltra, Dr. B. Escuder  
Departament de Química Inorgànica i Orgànica  
Universitat Jaume I, 12071 Castelló (Spain)  
E-mail: escuder@uji.es

[b] Dr. J. Nanda, A. Chotera, Prof. G. Ashkenasy  
Department of Chemistry  
Ben-Gurion University of the Negev, Be'er Sheva (Israel)  
E-mail: gonenash@bgu.ac.il

Supporting information for this article can be found under  
<http://dx.doi.org/10.1002/chem.201600344>.



Scheme 1. Structures of peptides.

analyze the coupling of C2/C3 fragments leading to small carbohydrates, such as tetroses and pentoses.<sup>[8]</sup> At the end of the paper, we thus show the utility of these new fibrillar networks in enhancing the synthesis of simple carbohydrate precursors.

## Results and Discussion

To study the effect of fibril structure and gel formation on catalysis, a new series of short lipophilic peptides equipped with L-proline amino acids at their N-terminus was prepared (1–6; Scheme 1).<sup>[9]</sup> Proline is known as a versatile organocatalyst for C–C forming reactions such as aldol and 1,4-conjugated addition reactions.<sup>[10]</sup> Additionally, the alternating sequence phenylalanine (F)–glutamic acid (E) has been chosen to facilitate the assembly of the peptides into  $\beta$ -sheet structures.<sup>[7a,11]</sup> We have recently shown that closely related structures, including alternating non-polar (aromatic)–polar (carboxylate) sequences, are prone to assemble into  $\beta$ -sheet structures and also form extended non polar aromatic regions that are able to bind hydrophobic guests.<sup>[12]</sup> Two types of alternating sequences have been designed, in which the amino acid neighboring proline is either the F or E, to test their effect on the catalytic results. Our previous experiments with related dipeptides have highlighted a hydrophobic residue located near the catalytic site to be selective for hydrophobic substrates.<sup>[9b]</sup> The short peptides in Scheme 1, compounds 1–4, present alkyl tails at the C-terminus, which decrease their solubility in water. Compounds 5 and 6 are deca-peptides presenting longer alternating sequences but lacking the hydrophobic tails.

### Self-assembly studies

Supramolecular structures produced by the self-assembly of peptides 1–6 were thoroughly characterized by various techniques, with the main purpose to later on correlate their structural features with the observed catalysis. Compounds 1 and 3, possessing the short C3 alkyl chains, were soluble under the conditions used for catalysis (phosphate buffer 0.1 M, pH 7) and were taken as non-assembling model compounds for cata-

lytic studies. Compounds 2 and 4 having longer alkyl chains were hardly soluble in aqueous solutions, and their solubility in water could not be precisely determined because it was below the detection limit of <sup>1</sup>H NMR spectroscopy. Compound 2 forms translucent hydrogels after dissolution under heating and cooling to RT at 1.5 mM, whereas dissolution of compound 4 in such processes leads to a milky suspension (Figure 1). Self-assembly studies of peptides 5 and 6, possessing longer sequences but no alkyl tails (in 0.5 M phosphate buffer, pH 7), have shown that both compounds form hydrogels at higher concentrations ( $\geq 7.5$  mM).

The microscopic morphology of these aggregates was further studied by TEM, Cryo-TEM, and AFM (Figure 2). The measurements revealed that the hy-

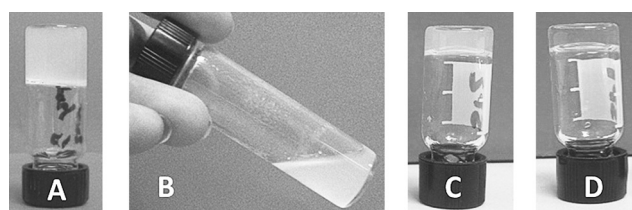
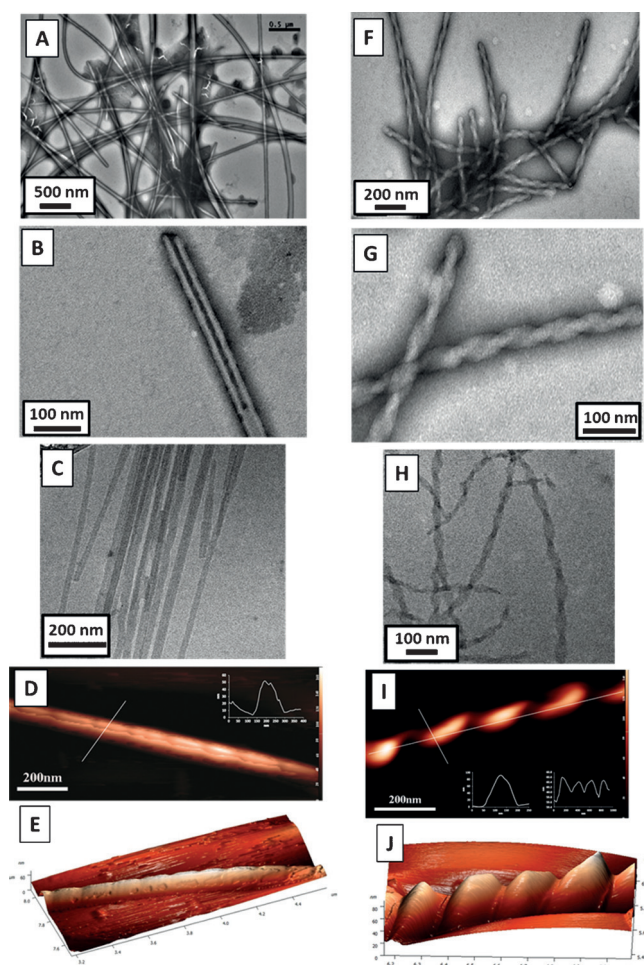


Figure 1. Macroscopic aspect of aggregates of compounds 2 (A, 1.5 mM), 4 (B, 1.5 mM), 5 (C, 7.5 mM) and 6 (D, 7.5 mM).

drogel of compound 2 was formed by the entanglement of long rigid tubes of about 30 nm in diameter and 10 nm of wall thickness (Figure 2B). AFM images suggest that these tubes can be formed by the folding of flat nanostructures (nanobelts or nanoribbons) into closed nanotubes (Figure 2D and 2E), as previously reported for similar self-assembled peptide amphiphiles.<sup>[13]</sup> Wide angle X-ray diffraction (WAXD) on freeze-dried xerogel (the Supporting Information, Figure S56A) revealed the presence of multiple diffraction peaks, following a periodicity typical of a lamellar structure, with a low angle diffraction at 36.5 Å assignable to the width of an interdigitated bilayer. On the other hand, aggregates of compound 4 formed a mesh of helical fibers that was not able to percolate the solution into a gel. These latter fibers of 50–70 nm in diameter present left-handed twists with a pitch of about 100 nm (the Supporting Information, Figure 2F–2J). In this case, WAXD of the freeze-dried xerogel (the Supporting Information, Figure S56B) showed a lower degree of crystallinity compared to that of the previous compound and a shorter low-angle diffraction at 28.7 Å.

The molecular arrangement within the different aggregates was also probed by circular dichroism (CD) (Figures S2–S5 in the Supporting Information). The CD spectrum of aggregated compound 2 revealed a Cotton effect typical to the  $\beta$ -sheet secondary structure, with a positive lobe at 208 nm, zero-crossing at 217 nm and a negative lobe minimum at 227 nm. These values appear slightly redshifted relative to the usual amide spectrum in  $\beta$ -sheet structures, probably indicating a twist



**Figure 2.** Morphology of aggregates formed by compound **2** (A–E) and compound **4** (F–J) at 1.5 mM obtained by TEM (A,B,F,G), Cryo-TEM (C,H), and AFM (D,E,I,J).

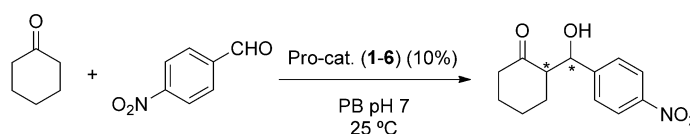
when the bilayer is closed into a nanotube.<sup>[14]</sup> Aggregates of compound **4** showed a different CD spectrum with two less intense negative peaks at 213 nm and 230 nm. This difference may be attributed to a stronger degree of  $\beta$ -sheets twist within the nanohelices (the Supporting Information, Figure S3). FTIR of the xerogels affords additional information regarding the H-bond networks present in the assemblies (the Supporting Information, Figure S19). The spectra of both compounds **2** and **4** showed a broad absorption band above  $2500\text{ cm}^{-1}$ , corresponding to the O–H stretching vibrations of associated carboxylic acids. However, these spectra revealed differences in bands related to the strength of H-bonding. The bands corresponding to the amide N–H and C=O stretching vibrations and to the carboxylic acid C=O stretching vibration appear at lower wavenumbers in the case of compound **2** ( $3284$  and  $1642\text{ cm}^{-1}$  (broad, amide, and carboxylic acid C=O stretching)) than for compound **4** ( $3332$ ,  $1675$ , and  $1646\text{ cm}^{-1}$ ). This difference reflects a lower extent of  $\beta$ -sheet H-bonding for compound **4**, in agreement with the twisting observed in its fibrils.

In the case of the hydrogels formed by compounds lacking the alkyl tail, TEM images showed

again a fibrillar aspect. Compound **5** showed straight and long fibers of about 30 nm in diameter (the Supporting Information, Figure S1 A,B). However, the resolution of the measurements did not allow the identification of tubes, as with analogue **2**. Compound **6** presented longer and more flexible, about 20 nm wide, fibers (the Supporting Information, Figure S1 C,D). At high magnification, some of these fibers displayed helical structures, albeit less defined than compound **4**, confirming the tendency of the PEF sequence to adopt highly twisted supramolecular arrangements. CD spectra of aggregated samples of **5** and **6** at 7.5 mM showed an intense negative band at 235 nm (the Supporting Information, Figure S5). In this case, the effect of sequence changes on the supramolecular structure was not as evident as with the short analogues. This observation supports the hypothesis that strong supramolecular effects result from competition between the hydrophobicity-driven packing of the alkyl-tail regions and the H-bonding in  $\beta$ -sheet regions. These two competing pathways modulate the supramolecular arrangements in assemblies of **2** and **4**, but are not significant in the case of the decapeptide analogues. A similar effect has been recently reported by Stupp et al. for small PAs with alternating hydrophilic (E) and hydrophobic (V) amino acids.<sup>[14]</sup> CD spectra of diluted samples of compounds **5** and **6** and of soluble analogues PFEC3 (**1**) and PEFC3 (**3**) displayed bisignate bands with negative lobes at about 210 nm and positive lobes at about 220 nm, corresponding to the molecular CD associated with intramolecularly folded conformations (see the Supporting Information, Figures S2 and S4 for CD spectra and S7 for calculated models of folding). In summary, it is remarkable that minor changes in the amino acid sequence, or elimination of the C-terminus alkyl chain, strongly influence the aggregation tendency and furthermore result in a significant difference in self-assembly packing and microscopic architectures.

### Catalysis

The catalytic activity of peptides **1–6** was tested towards the aldol coupling of cyclohexanone and 4-nitro-benzaldehyde as a benchmark reaction (Scheme 2). This reaction has been previously studied, displaying an excellent test for the catalytic activity of hydrophobic aggregates in water.<sup>[8]</sup> In the current work, a 10% loading of catalyst and 10 equivalents of cyclohexanone per aldehyde equivalent were employed, and the reaction was run at  $25\text{ }^{\circ}\text{C}$  and buffered at pH 7 (phosphate buffer; PB). Results appear collected in Table 1. As can be seen, the use of soluble catalysts **1** and **3** did not lead to significant aldol product yields even after 72 h (Table 1, entries 2 and 4), and the outcomes of these reactions were comparable to that



**Scheme 2.** Direct aldol reaction.

**Table 1.** Catalytic results for the aldol reaction using compounds 1–6 as catalysts.<sup>[a]</sup>

Entry	Catalyst	t [h]	Yield <sup>[b]</sup> [%]	d.r. <sup>[b]</sup> ( <i>syn/anti</i> )	e.r. <sup>[c]</sup> ( <i>anti</i> )
1	–	72	14	–	–
2	1	72	32	15:85	n.d.
3	2	72	>99	14:86	12:88
4	3	72	17	18:82	n.d.
5	4	72	>99	20:80	12:88
6	1	15	9	15:85	–
7	2	15	>99	15:85	–
8	3	15	6	20:80	–
9	4	15	>99	9:91	–
10	2	2	93	8:92	–
11	4	2	51	15:85	–
12	2	1	83	10:90	–
13	4	1	32	14:86	–
14	5	72	85	15:85	12:88
15	6	72	50	16:84	20:80

[a] Catalytic conditions for compounds 1–4:  $6.5 \times 10^{-3}$  mmol of catalyst (10%) and 10 equiv of cyclohexanone in 2 mL of phosphate buffer 0.1 M at pH 7 and 25 °C. For compounds 5 and 6:  $6.5 \times 10^{-3}$  mmol of catalyst (10%) and 10 equiv of cyclohexanone in 0.5 mL of phosphate buffer 0.5 M at pH 7 and 25 °C. [b] Yields and diastereoisomer ratios were determined by <sup>1</sup>H NMR spectroscopy. [c] Enantiomer ratios were determined by chiral HPLC.

of reactions in control experiments without a catalyst (entry 1). Remarkably, when self-assembled catalysts 2 and 4 were used, a quantitative conversion of the aldehyde was obtained after the same reaction period (Table 1, entries 3 and 5). Shortening the reaction time revealed a difference in reaction rates between these two active assemblies (Figure 3). For example, after 2 h, the aldol yield was 93% for reactions catalyzed by 2 (Table 1, entry 10), whereas for reactions with catalyst 4 it was only 51% (entry 11).

Decapeptides 5 and 6 were also studied as catalysts, and it was observed that reactions in the presence of these compounds were significantly slower than in the presence of the tripeptide analogues 2 and 4; even after 72 h, substrate conversion was not yet complete (Table 1, entries 14 and 15).

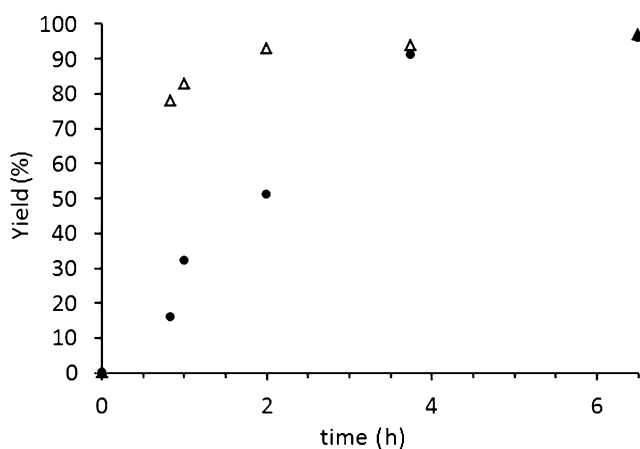


**Figure 3.** Yield of the aldol reactions as a function of time in the presence of self-assembled catalysts 2 (Δ) and 4 (●).

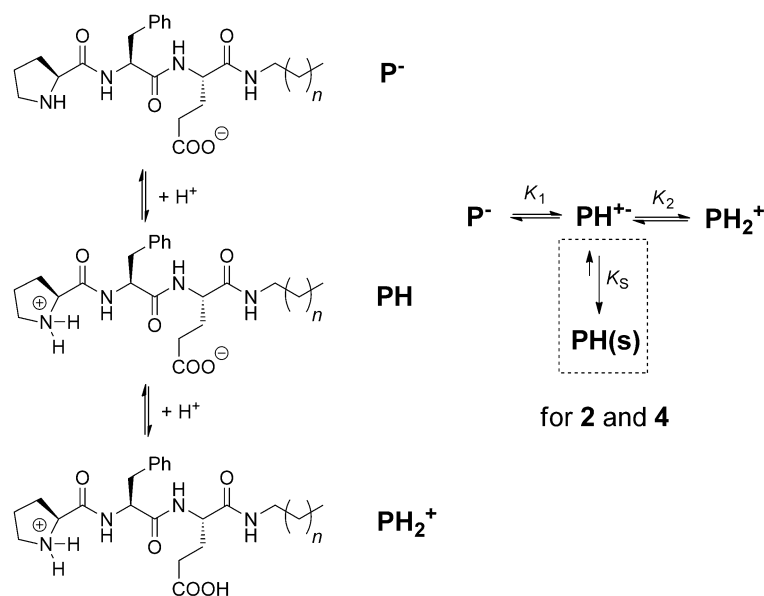
## Mechanistic studies

Various examples have been previously published demonstrating that simple amino acids and peptides can serve as organo-catalysts for direct “in water” and “on water” aldol reactions.<sup>[16]</sup> However, although reports have appeared for such reactions using emulsions and suspensions of catalysts in water, in most of the cases the relationship between the supramolecular structure of the aggregates and the catalysis was not investigated, thus ignoring the paramount effects that may appear after self-assembly.<sup>[17]</sup> However, it is important to fully understand the structural characteristics of the catalytic sites and to clarify the role of self-assembly on the catalytic properties of the system. The catalytic mechanism for proline-based catalysts has been shown to proceed by the formation of an enamine intermediate between the catalyst and the ketone. Afterwards, the prolyl-enamine participates in the nucleophilic addition to the aldehyde. Therefore, it is important that the proline amino group remains in its non-protonated form under the catalytic conditions. For that reason, pH titration experiments have been performed to identify the catalyst species at pH 7 (see Figures S15 and S16 in the Supporting Information). Titrations of compounds 1–4 have been performed by starting from basic solutions that showed no precipitation or gelation, and then proceeding with subsequent slow addition of acid aliquots until an acidic final pH was reached. A general Scheme for the different steps along this process is shown in Scheme 3, and the resulting protonation constant values are collected in Table 2.

**Table 2.**  $pK_a$  values for compounds 1–4 determined by potentiometric titrations.

Catalyst	$pK_1$	$pK_2$
1	$8.22 \pm 0.02$	$4.34 \pm 0.02$
2	$9.72 \pm 0.03$	$6.85 \pm 0.04$
3	$8.27 \pm 0.02$	$4.21 \pm 0.04$
4	$7.60 \pm 0.01$	$6.92 \pm 0.01$

In the case of compounds 1 and 3, which are soluble for the entire pH range, the values for  $pK_1$  are 8.22 and 8.27, respectively, meaning that at pH 7 the predominant species would be a zwitterion ( $PH^{+-}$  in Scheme 2). As a consequence, the proline residue would be protonated and not available for the enamine-based catalysis. On the other hand, compounds 2 and 4 bearing a C12 alkyl tail are much more hydrophobic, and their molecular species at neutral pH tend to aggregate into a hydrogel and a sticky suspension, respectively (PH in Scheme 2). It is therefore reasonable to propose that in these latter aggregates, which are formed by neutral non-charged molecules as confirmed by the presence of  $-COOH$  bands in the FTIR spectra of freeze dried samples of aggregated 2 and 4 (the Supporting Information, Figure S19), the proline residues are readily available to react with the substrates. The formation of these aggregates has an effect on the  $pK_1$  values, which are 9.72 and 7.60 for 2 and 4, respectively.<sup>[18]</sup> However, both com-



**Scheme 3.** pH-dependent speciation exemplified for compounds **1** and **2**. Inset: detailed diagram including equilibrium constants valid for compounds **1–4**.

pounds are strongly aggregated at pH 7 and, as can be seen in the speciation diagram, at pH 7 the amount of the active species PH is of 60% for compound **2** and 40% for compound **4** in pure water. Moreover, the catalytic experiments are performed in phosphate buffer that causes a dramatic decrease of the solubility due to the so-called Hofmeister effect,<sup>[19]</sup> as the phosphate ion belongs to the group of ions that usually lower the solubility of hydrophobic solutes in water, termed kosmotropic ions.<sup>[20]</sup> For the studied case, this effect is strongly active for both compounds **2** and **4**. Indeed, the <sup>1</sup>H NMR spectra of the two compounds in buffer at pH 7 did not show any signal corresponding to free compounds, revealing that the soluble fraction of both falls below the detection limit of this technique (<5%), and therefore >95% of the catalyst molecules are in the non-protonated active form at that pH (the Supporting Information, Figures S17 and S18). All these data clearly show that proline amino groups are non-protonated and ready to react with electrophiles under the conditions used for the catalytic experiments.

To understand the observed difference between the catalytic activity of compounds **2** and **4**, we then decided to study the accessibility of the substrates to the catalytic sites. Therefore, an experiment was set up in which samples of self-assembled catalysts and a smaller excess of cyclohexanone (2.5 equiv) were prepared, and the amount of cyclohexanone incorporated into the aggregated phase was quantified by <sup>1</sup>H NMR spectroscopy (see the Supporting Information for details). Cyclohexanone is significantly soluble in aqueous solution and would only be incorporated into the aggregates if it reacts with a proline residue forming an enamine. Interestingly, it was observed that one equivalent of cyclohexanone was incorporated into the gel formed by catalyst **2**, whereas aggregates of catalyst **4** only entrapped 0.5 equiv of this ketone. This suggests that catalytic sites of compound **2** are more accessible to cyclohexanone than those of catalyst **4**.

Kinetic studies were performed to analyze a possible enzyme-like mechanism. Catalytic experiments were performed by keeping the catalyst concentration constant and varying the total concentration of substrate (at constant cyclohexanone/aldehyde ratio). The observed kinetics did not follow the typical Michaelis–Menten velocity profile, and therefore rules out the formation of a pre-organized catalyst–substrate complex (Figures S20 and S21 in the Supporting Information).

On the other hand, *p*-nitrobenzaldehyde is poorly soluble in water, and therefore should be incorporated into the hydrophobic regions of the gel phase to get access to the catalytic center and react with the enamine intermediate. 1-Anilino-naphthalene-8-sulphonate (ANS), a fluorescent probe extensively used to track hydrophobic regions in proteins, was employed to reveal the hydrophobicity of the aggregates.<sup>[21]</sup> A fluorescence blueshift is expected upon ANS binding, along with an increase in the fluorescence intensity, due to an increase in the rigidity of the probe within the hydrophobic pockets. As can be seen in Figure S22 (the Supporting Information), a fluorescence emission band appears at about 460 nm in the spectrum of both compounds **2** and **4**, blueshifted from the weak emission of the blank solution at 490 nm. This band, which is more intense for compound **4** than for compound **2**, corroborates the presence of hydrophobic regions. In the case of compounds **5** and **6**, the two compounds present a catalytic residue similar to compounds **1–4**, but they present longer sequences and do not bear alkyl tails at the C-terminus. The ANS binding assays performed for compounds **5** and **6** in comparison with those of compounds **2** and **4** revealed a significantly lower hydrophobicity. On the other hand, the amount of incorporated cyclohexanone was also quantified for these compounds using <sup>1</sup>H NMR spectroscopy, showing that less than 0.1 equiv of cyclohexanone did react. These two results support the explanation that the slower catalysis rate observed for **5** and **6**, compared with **2** and **4**, is due to a combi-

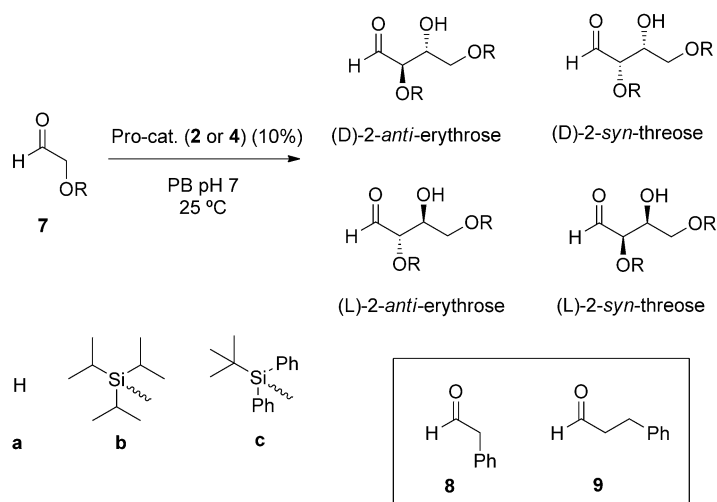
nation of poor accessibility of both reagents to the catalytic fibers.

Remarkably, a difference in catalytic performance related to the peptide sequence could be observed again in favor of compound **5**, which contains a phenylalanine residue next to proline. This general trend suggests that F plays a role in catalysis, probably through secondary interactions at the transition state of the reaction. It has to be mentioned that sequence variations did not affect significantly the stereoselectivity of the reactions. In all experiments, diastereomeric ratios *syn/anti* were in the range 10:90 to 20:80, and enantiomer ratios for the *anti* product were about 10:90. These facts support the hypothesis that there is no specific substrate binding close to the catalytic site but a preferential partitioning of the substrates into the hydrophobic region of the gel fibers that is key to the acceleration of the reaction, a trend that is also observed in micellar catalysis.<sup>[5]</sup>

### Biomimetic catalysis

At this point, the emergence of catalytic activity through peptide self-assembly has been established, and a further step is taken towards catalysis of biologically relevant aldol product formation. Taking Nature as an inspiration, aldol reactions can be used to obtain carbohydrate derivatives.<sup>[22]</sup> Aldolase I uses catalytic enamine activation in the metabolic biosynthetic pathways of carbohydrates. For instance, dihydroxyacetone phosphate (DHP) is activated for the subsequent coupling with C2 or C3 aldehydes, leading to either tetroses or pentoses, respectively.

In this context, the relevance of organocatalysis in water, and in particular proline catalysis, for the prebiotic origin of carbohydrates, is evident and has been highlighted by several authors.<sup>[23]</sup> Therefore, we decided to study the hydrogels and aggregates formed by compounds **2** and **4** as catalysts for the self-condensation of several  $\alpha$ -oxy-aldehydes and phenylalkyl aldehydes (Scheme 4). Firstly, 2-hydroxyacetaldehyde deriva-



Scheme 4. Self-condensation of aldehydes.

Table 3. Catalytic results for the self-condensation of aldehydes **7a–c** and **9**.<sup>[a]</sup>

Entry	Catalyst	Aldehyde	t [h]	Aldol yield [%] <sup>[b]</sup>
1	<b>2</b>	<b>7a</b>	48	< 5
2	<b>4</b>	<b>7a</b>	48	< 5
3	<b>2</b>	<b>7b</b>	15	> 95 <sup>[c]</sup>
4	<b>4</b>	<b>7b</b>	15	> 95 <sup>[c]</sup>
5	<b>2</b>	<b>7c</b>	2	84 <sup>[d]</sup>
6	<b>4</b>	<b>7c</b>	2	50 <sup>[d]</sup>
7	<b>2</b>	<b>7c</b>	15	92
8	<b>4</b>	<b>7c</b>	15	76
9	<b>2</b>	<b>9</b>	2	17
10	<b>4</b>	<b>9</b>	2	2
11	<b>2</b>	<b>9</b>	15	57
12	<b>4</b>	<b>9</b>	15	24

[a] Catalytic conditions:  $6.5 \times 10^{-3}$  mmol of catalyst (4.37 mg, 10%) and  $6.5 \times 10^{-2}$  mmol of the corresponding aldehyde in 2 mL of phosphate buffer 0.1 M at pH 7 and 25 °C. [b] Yields and diastereomeric ratio are determined by <sup>1</sup>H NMR spectroscopy (see the Supporting Information). [c] Mixture of compounds, see text. [d] d.r. (*syn/anti*), 10:90, e.r. *anti* product 91:9, determined as reported in ref. [22], see the Supporting Information for details.

tives (**7a–c**) were studied as substrates leading to tetrose-based products.<sup>[24]</sup> Results appear collected in Table 3.

Unprotected 2-hydroxyacetaldehyde (**7a**) did not react in the presence of any of the self-assembled catalyst, even after a long reaction time (Table 3, entries 1 and 2). However, the reaction was accomplished quite fast when the  $\alpha$ -hydroxyl group was protected as a silyl ether (**7b**, **7c**). The inactivity of self-assembled catalysts against polar substrates has been observed earlier for related systems, and supports the fact that a hydrophobic environment of the fibers is required to dissolve/store the reagent near the catalytic site.<sup>[9b]</sup> Triisopropylsilyl (TIPS)-protected glycolaldehyde (**7b**) reacted as previously described by Clarke et al., leading to mixtures of aldols together with a trimeric acetal (see Figure S10 in the Supporting Information).<sup>[17b]</sup> However, different results were obtained for reactions of *tert*-butyldiphenylsilyl (TBDPS)-protected analogue **7c**. In this case, using self-assembled catalysts **2** and **4**, considerable yields of aldol were already obtained after a few hours of reaction. Again, the best results in terms of rate appeared for catalyst **2**, with a yield of 80% after 2 h of reaction, compared with 50% obtained for catalyst **4**. Moreover, the aldehyde-containing products did not participate in further aldol reactions for both catalysts (see Figure S11 in the Supporting Information). It seems that the presence of aromatic fragments in substrate and F residues in the catalyst play a role that favors the aldol product. The major product of the reaction was determined to be the L-2-*anti*-erythrose derivative, revealing a remarkable stereoselectivity (d.r. 90:10, enantiomeric ratio (e.r.) 91:9).

In addition to the study of hydroxyacetaldehyde derivatives, 2-phenyl acetaldehyde (**8**) and 3-phenyl propionaldehyde (**9**) were used as substrates, testing

the role of the  $\alpha$ -oxy group. When studying aldehyde **8**, a complex mixture of products was observed in  $^1\text{H}$  NMR analysis of the crude, showing multiple aldehyde C–H singlets between  $\delta = 9$  and 10 ppm (not shown in Table 3; see Figure S12 in the Supporting Information). Furthermore, an analysis of this crude material by ESI-MS revealed the presence of different peaks corresponding to poly-condensation products. In the case of aldehyde **9**, the main reaction product was the dehydrated aldol (see Table 3, entries 9–12 and Figure S10 in the Supporting Information). For both aldehydes, using either **2** or **4** as catalyst, the rates of reaction were slower than for the  $\alpha$ -oxy-analogues. Nevertheless, from a prebiotic chemistry point of view, these condensation reactions resulted in the formation of polyaldols, potential precursors of larger carbohydrates and polyketide natural products.<sup>[24]</sup>

## Conclusion

We have presented here an example of the emergence of catalytic activity through the self-assembly of short peptides in water. Although the use of peptides in catalysis is widely reported, in particular the so-called “on-water” reactions, we were able to further rationalize here the catalytic activity in terms of the supramolecular structure of the system, which is not generally considered in the field of organocatalysis.

We have shown that the formation of aggregates is fundamental for the development of catalytic activity by comparing the assembling compounds **2** and **4** with the soluble analogues **1** and **3**. Moreover, we have determined that there is a relationship between the amino acid sequence, the supramolecular and microscopic organization of the material, and the accessibility of the substrates to the reaction site. Additionally, the presence of hydrophobic fragments and especially alkyl tails has been shown to help in the solubilization of the hydrophobic substrates and improve their catalytic performance; compounds **5** and **6** lacking these tails had a reduced catalytic efficiency. It is noteworthy to remark that these functional materials are formed by simple molecules with pre-programmed information, which is in turn translated into complex catalytic systems solely through noncovalent interactions. In this sense, catalytic self-assembled peptides could be considered as supramolecular protein-like functional materials.

Finally, it is important to highlight that C–C bond-forming reactions such as aldol condensations are of great value because they increase molecular complexity and structural diversity in one simple step. The results presented here are thus relevant in the context of prebiotic chemistry. Probable prebiotic scenarios for the synthesis of small peptides have thus been proposed. In combination with the role of self-assembly, both the formation of compartments and the emergence of catalysis, they point to a plausible pathway towards the appearance of chemical complexity.<sup>[25]</sup> In this context, catalytic self-assembled peptides can be seen as intermediate evolutionary systems, between simple soluble molecular catalysts and complex protein entities, namely, the enzymes.

## Acknowledgements

This work was supported by the Ministry of Economy and Competitiveness of Spain (Grant CTQ2012-37735) and Universitat Jaume I (Grant P1-1B2013-57). M.T.-S. thanks the Ministry of Education, Culture and Sport of Spain for an FPU fellowship. J.N. thanks the PBC program for post-doctoral fellowship. We acknowledge the COST actions CM1005 and CM1304. We thank Dr. N. Wagner (BGU) for help in editing the manuscript.

**Keywords:** aldol reaction • gels • peptides • self-assembly • supramolecular chemistry

- [1] a) J. M. Lehn, *Proc. Natl. Acad. Sci. USA* **2002**, *99*, 4763; b) A. Mulder, J. Huskens, D. N. Reinhoudt, *Org. Biomol. Chem.* **2004**, *2*, 3409; c) J. D. Badjic, A. Nelson, S. J. Cantrill, W. B. Turnbull, J. F. Stoddart, *Acc. Chem. Res.* **2005**, *38*, 723; d) L. C. Palmer, Y. S. Velichko, M. Olvera de La Cruz, S. I. Stupp, *Phil. Trans. RSC A: Math. Phys. Eng. Sci.* **2007**, *365*, 1417; e) A. Barnard, D. K. Smith, *Angew. Chem. Int. Ed.* **2012**, *51*, 6572; *Angew. Chem.* **2012**, *124*, 6676; f) C. Fasting, C. A. Schalley, M. Weber, O. Seitz, S. Hecht, B. Kocsch, J. Dornedde, C. Graf, E.-W. Knapp, R. Haag, *Angew. Chem. Int. Ed.* **2012**, *51*, 10472; *Angew. Chem.* **2012**, *124*, 10622; g) J. M. Lehn, *Angew. Chem. Int. Ed.* **2013**, *52*, 2836; *Angew. Chem.* **2013**, *125*, 2906.
- [2] a) D. Deamer, S. Singaram, S. Rajamani, V. Kompanichenko, S. Guggenheim, *Phil. Trans. R. Soc. B* **2006**, *361*, 1809; b) K. Kunihara, M. Tamura, K. Shohda, T. Toyota, K. Suzuki, T. Sugawara, *Nat. Chem.* **2011**, *3*, 775; c) A. J. Dzieciol, S. Mann, *Chem. Soc. Rev.* **2012**, *41*, 79; d) K. Adamala, J. W. Szostak, *Nat. Chem.* **2013**, *5*, 495; e) X. Huang, M. Li, D. C. Green, D. S. Williams, A. J. Patil, S. Mann, *Nat. Commun.* **2013**, *4*, 2239; f) P. Wade, H. Umakoshi, P. Stano, F. Mavelli, *Chem. Commun.* **2014**, *50*, 10177; g) X. Huang, A. J. Patil, M. Li, S. Mann, *J. Am. Chem. Soc.* **2014**, *136*, 9225.
- [3] W. S. Childers, R. Ni, A. K. Mehta, D. G. Lynn, *Curr. Opin. Chem. Biol.* **2009**, *13*, 652.
- [4] A. M. Brizard, J. H. van Esch, *Soft Matter* **2009**, *5*, 1320.
- [5] For a review on catalytic micelles see: T. Dwars, E. Paetzold, G. Oehme, *Angew. Chem. Int. Ed.* **2005**, *44*, 7174–7199; *Angew. Chem.* **2005**, *117*, 7338–7364.
- [6] For recent examples of catalytic peptide fibers see: a) M. O. Guler, S. I. Stupp, *J. Am. Chem. Soc.* **2007**, *129*, 12082; b) F. Rodríguez-Llansola, B. Escuder, J. F. Miravet, *J. Am. Chem. Soc.* **2009**, *131*, 11478; c) Z. P. Huang, S. W. Guan, Y. G. Wang, G. N. Shi, L. N. Cao, Y. Z. Gao, Z. Y. Dong, J. Y. Xu, Q. Luo, J. Q. Liu, *J. Mater. Chem. B* **2013**, *1*, 2297–2304; d) C. M. Rufo, Y. S. Moroz, O. V. Moroz, J. Stöhr, T. A. Smith, X. Hu, W. F. DeGrado, I. V. Korendovych, *Nat. Chem.* **2014**, *6*, 303; e) C. Zhang, X. Xue, Q. Luo, Y. Li, K. Yang, X. Zhuang, Y. Jiang, J. Zhang, J. Liu, G. Zou, X.-J. Liang, *ACS Nano* **2014**, *8*, 11715; f) N. Singh, M. P. Conte, R. V. Ulijn, J. F. Miravet, B. Escuder, *Chem. Commun.* **2015**, *51*, 13213; g) M. Bélières, N. Chouini-Lalanne, C. Dejugnat, *RSC Adv.* **2015**, *5*, 35830; h) K. S. Lee, J. R. Parquette, *Chem. Commun.* **2015**, *51*, 15653; i) N. Singh, M. Tena-Solsona, J. F. Miravet, B. Escuder, *Isr. J. Chem.* **2015**, *55*, 711; j) K. L. Duncan, R. V. Ulijn, *Bio-catalysis* **2015**, *1*, 67.
- [7] a) B. Rubinov, N. Wagner, H. Rapaport, G. Ashkenasy, *Angew. Chem.* **2009**, *121*, 6811; b) J. M. A. Carnall, C. A. Waudby, A. M. Belenguer, M. C. A. Stuart, J. J. P. Peyralans, S. Otto, *Science* **2010**, *327*, 1502; c) B. Rubinov, N. Wagner, M. Matmor, O. Regev, N. Ashkenasy, G. Ashkenasy, *ACS Nano* **2012**, *6*, 7893.
- [8] J. L. Tymoczko, J. M. Berg, L. Stryer, *Biochemistry: a Short Course*, 2nd ed., W. H. Freeman and Co., New York, **2013**.
- [9] a) F. Rodríguez-Llansola, J. F. Miravet, B. Escuder, *Chem. Commun.* **2009**, 7303; b) C. Berdugo, J. F. Miravet, B. Escuder, *Chem. Commun.* **2013**, *49*, 10608.
- [10] B. List in *Modern Aldol Reactions, Vol. 1* (Ed.: R. Mahrwald), Wiley-VCH, Weinheim, **2004**, p. 161.
- [11] a) H. Rapaport, K. Kjaer, T. R. Jensen, L. Leiserowitz, D. A. Tirrell, *J. Am. Chem. Soc.* **2000**, *122*, 12523; b) N. R. Lee, C. J. Bowerman, B. J. Nilsson,

- Pept. Sci.* **2013**, *100*, 738; c) Y. Raz, B. Rubinov, M. Matmor, H. Rapaport, G. Ashkenasy, Y. Miller, *Chem. Commun.* **2013**, *49*, 6561.
- [12] a) M. Tena-Solsona, J. F. Miravet, B. Escuder, *Chem. Eur. J.* **2014**, *20*, 1023; b) M. Tena-Solsona, S. Alonso-de Castro, J. F. Miravet, B. Escuder, *J. Mater. Chem. B* **2014**, *2*, 6192.
- [13] See for instance: a) T. Shimizu, M. Masuda, H. Minamikawa, *Chem. Rev.* **2005**, *105*, 1401; b) L. Ziserman, H.-Y. Lee, S. R. Raghavan, A. Mor, D. Danino, *J. Am. Chem. Soc.* **2011**, *133*, 2511; c) T. G. Barclay, K. Constantopoulos, J. Matison, *Chem. Rev.* **2014**, *114*, 10217.
- [14] a) E. T. Pashuck, H. Cui, S. I. Stupp, *J. Am. Chem. Soc.* **2010**, *132*, 6041; b) E. T. Pashuck, S. I. Stupp, *J. Am. Chem. Soc.* **2010**, *132*, 8819.
- [15] H. Cui, A. G. Cheetham, E. T. Pashuck, S. I. Stupp, *J. Am. Chem. Soc.* **2014**, *136*, 12461.
- [16] E. A. C. Davie, S. M. Mennen, Y. Xu, S. J. Miller, *Chem. Rev.* **2007**, *107*, 5759.
- [17] a) N. Mase, Y. Nakai, N. Ohara, H. Yoda, K. Takabe, F. Tanaka, C. F. Barbas, *J. Am. Chem. Soc.* **2006**, *128*, 734; b) L. Burroughs, P. A. Clarke, H. Forintos, J. A. R. Gilks, C. J. Hayes, M. E. Vale, W. Wade, M. Zbytniewski, *Org. Biomol. Chem.* **2012**, *10*, 1565; c) J. Duschmalé, S. Kohrt, H. Wennemers, *Chem. Commun.* **2014**, *50*, 8109.
- [18] There is an intriguing effect of aggregation on  $pK_a$  values of compounds **2** and **4**. The relationship between the structure of aggregates and  $pK_a$  values is currently under study. For recent examples on peptide aggregation effects on  $pK_a$ , see, for instance: C. Tang, A. M. Smith, R. F. Collins, R. V. Ulijn, A. Saiani, *Langmuir* **2009**, *25*, 9447.
- [19] V. J. Nebot, J. J. Ojeda-Flores, J. Smets, S. Fernández Prieto, B. Escuder, J. F. Miravet, *Chem. Eur. J.* **2014**, *20*, 14465.
- [20] a) P. Lo Nostro, B. W. Ninham, *Chem. Rev.* **2012**, *112*, 2286; b) P. Lo Nostro, A. Lo Nostro, B. W. Ninham, G. Pesavento, L. Fratoni, P. Baglioni, *Curr. Opin. Colloid Interface Sci.* **2004**, *9*, 97.
- [21] a) E. Schönbrunn, S. Eschenburg, K. Luger, W. Kabsch, N. Amrhein, *Proc. Natl. Acad. Sci. USA* **2000**, *97*, 6345; b) G. Chadha, Y. Zhao, *J. Colloid Interface Sci.* **2013**, *390*, 151.
- [22] a) A. B. Northrup, D. W. C. MacMillan, *Science* **2004**, *305*, 1752; b) N. Mase, C. F. Barbas III, *Org. Biomol. Chem.* **2010**, *8*, 4043.
- [23] a) J. E. Hein, D. G. Blackmond, *Acc. Chem. Res.* **2012**, *45*, 2045; b) J. Mlynarski, B. Gut, *Chem. Soc. Rev.* **2012**, *41*, 587.
- [24] a) J. Rohr, *Angew. Chem. Int. Ed.* **2000**, *39*, 2847; *Angew. Chem.* **2000**, *112*, 2967; b) A. M. P. Koskinen, K. Karisalmi, *Chem. Soc. Rev.* **2005**, *34*, 677.
- [25] a) G. Danger, R. Plasson, R. Pascal, *Chem. Soc. Rev.* **2012**, *41*, 5416; b) K. Ruiz-Mirazo, C. Briones, A. de La Escosura, *Chem. Rev.* **2014**, *114*, 285.

Received: January 25, 2016

Published online on March 23, 2016